

# FT-IR Studies of Nickel Substituted Polycrystalline Zinc Spinel Ferrites for Structural and Vibrational Investigations

H. A. DAWOUD\*, L. ABU OUDA and S. K. K. SHAAT

Department of Physics, Faculty of Science, Islamic University,  
P.O. Box 108, Gaza, Palestine

hdawoud@iugaza.edu.ps

Received 1 September 2016 / Accepted 10 October 2016

**Abstract:** FT-IR spectra of  $\text{Ni}_{1-s}\text{Zn}_s\text{Fe}_2\text{O}_4$  spinel ferrite,  $s$  changed by 0.2 according to  $0.0 \leq s \leq 1.0$ , have been analyzed in the frequency range (350–1000)  $\text{cm}^{-1}$ . Six polycrystalline ferrites samples were synthesized using the conventional standard double sintering ceramic method. Two main absorption bands were observed, their positions were found to be strongly dependent on  $s$ -value. The high frequency band in the range 550-600  $\text{cm}^{-1}$  and a low frequency band at around 400  $\text{cm}^{-1}$  were assigned to tetrahedral  $T_d$  and octahedral  $O_h$  sites, respectively, of spinel lattice. Force constant ( $F_C$ ) was calculated for  $T_d$  and  $O_h$  sites and was found to decrease with increasing Zn ions. Threshold frequency  $\nu^{\text{th}}$  for the electronic transition was determined and found to increase with increasing Zn ions. Cations distribution for the prepared mixed ferrite was concluded based on the FT-IR spectra. The ionic radii for each site were correlated to the cations distribution of the given ferrite.

**Keywords:** Spinel, Ferrite, Nickel, Zinc, Cation

## Introduction

Spinel ferrites have been studied extensively due to easy synthesis and abundant uses in technological and industrial applications<sup>1</sup>. A general chemical formula of spinels is  $\text{DT}_2\text{O}_4$ , D and T is divalent and trivalent cations, respectively<sup>2-4</sup>. The generic structural formula or cations distribution of spinels can be expressed by  $(D_{1-s}T_s)_{\text{Tet.}}\{D_sT_{2-s}\}_{\text{Oct.}}O_4^{2-}$ , with  $0.0 \leq s \leq 1.0$  which is the inversion parameter (degree of inversion),  $( )_{\text{Tet.}}$  and  $\{ \}_{\text{Oct.}}$  are tetrahedral ( $T_d$ ) and octahedral ( $O_h$ ) sites, respectively<sup>5,6</sup>. Depending on cations distribution, spinel consists of three types of magnetic structures, they are; normal ( $S=0.0$ ), perfectly inverse ( $S=1.0$ ) and otherwise partially inverse or intermediate ( $0.0 < s < 1.0$ )<sup>5-7</sup>. The degree of inversion in the spinel lattice depends on ionic radii, ionic charge, electrostatic (Madelung) energy, electronic configuration, relative stabilization energies in the  $T_d$  and  $O_h$  fields, short-range

Born repulsion energy, crystal field effects and polarization effects<sup>6-9</sup>. For spinel ferrites with  $T = Fe^{3+}$  i.e.  $DFe_2^{3+}O_4^{2-}$ , the distribution of the different ions in the  $T_d$  and  $O_h$  sites mainly depends on the method of preparation and processing conditions<sup>10</sup>. The mixed polycrystalline soft spinel ferrites  $(Zn, Ni)Fe_2O_4$  have been intensely studied because of their remarkable high-frequency operation (1-100 GHz) as well as because of their favorable properties such as low eddy current losses and high of resistivity, permeability, Curie temperature and saturation magnetization in the radio frequency (RF) region<sup>11-14</sup>. Therefore, it plays a significant role in many applications<sup>1,11,13-19</sup>. The structure of  $(Zn, Ni)Fe_2O_4$  spinel ferrite belongs to a close-packed spinel face-centered cubic (fcc) with  $O_h^7(Fd3m)$  space group symmetry (Figure 1)<sup>6,17,20-22</sup>. In the present investigation, we are measured and discussed the fourier transformation infrared (FT-IR) spectra of mixed polycrystalline soft ferrites of cubic spinel structure  $Ni_{1-s}Zn_sFe_2O_4$  powders, where  $s = 0.0$  to  $1.0$  in step of  $0.20$ , which have been carried out by normal conventional ceramic method.

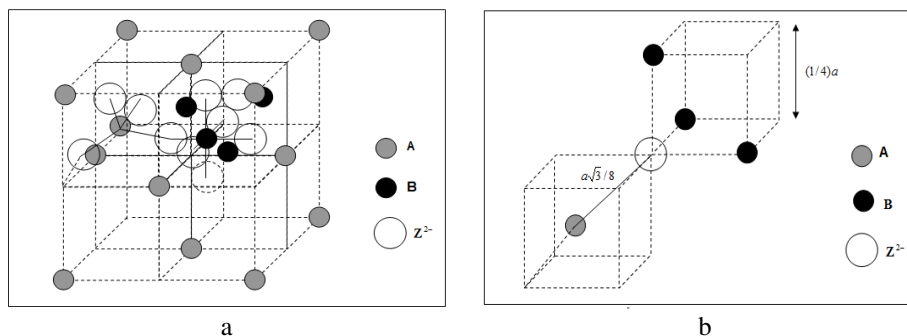
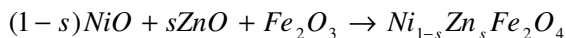


**Figure 1.** (a) Two octants of the unit cell of the spinel lattice structure. A and B ions are at  $T_d$  and  $O_h$  sites of the  $Z^{2-}$  anions packing. (b) An anion  $Z^{2-}$  in the spinel lattice structure with its nearest cations neighbors<sup>9</sup>.

## Experimental

The mixed polycrystalline ferrites  $Ni_{1-s}Zn_sFe_2O_4$ , where  $s$  is the percentage increment of  $Zn$  ions on the compound which have the value  $s = 0.0, 0.2, 0.4, 0.6, 0.8$  and  $1.0$ , were prepared by using the standard double sintering (SSR) by mixing pure metal oxides in the calculated proportions according to the formula



25.0 g from high purity metal oxides were used to prepare each composition of the investigated polycrystalline spinel ferrites. The metal oxides were weighed using a sensitive electric balance (ADAM model PW124) with an accuracy  $1 \times 10^4$  g. The weighed metal oxides were mixed and then grounded to a very fine powder for 5 h. The mixed powder of metal oxides was pre-sintered at  $750$  °C for 3 h soaking time using a laboratory Furnace (BIFATHERM model AC62). Then the prefired powder was well ground for 3 h and pressed with hydraulic press under constant pressure of  $3 \times 10^8$  pa. After that, samples were sintered at  $1200$  °C for soaking time of 5 h using a laboratory Furnace (BIFATHERM model A C62). After sintering process, the samples were cooled down gradually to room temperature.

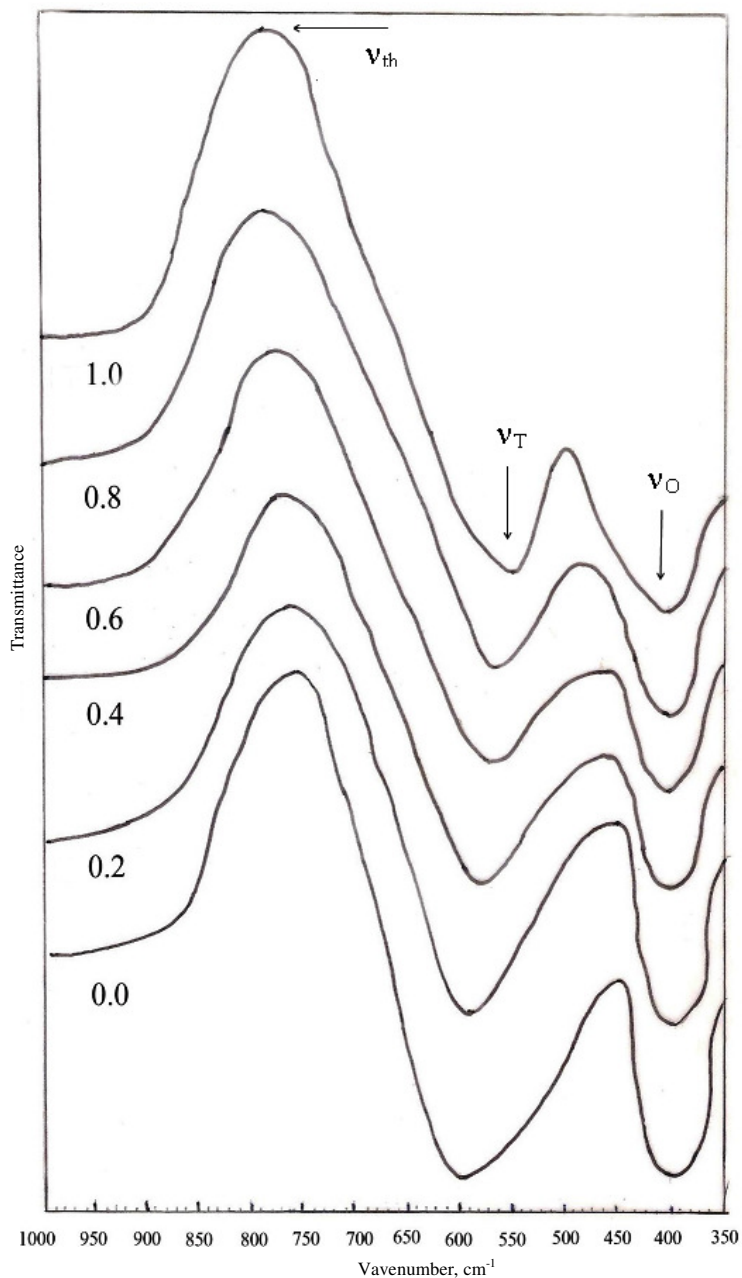
For recording FT-IR spectra, the powder of the samples was mixed with Potassium Bromide (KBr) at a ratio of 1:200 by weight to uniform dispersion in KBr pellet. The mixed powder of samples were pressed at  $3 \times 10^8$  pa by a hydraulic press. Clean discs with a thickness approximate of 1.0 mm were obtained. FT-IR spectra in the range from 350 to  $1000 \text{ cm}^{-1}$  were recorded in room temperature using FT-IR Spectrophotometer (Cary 660 FT-IR spectrometer).

## Results and Discussion

The FT-IR spectrometer technique is depended on that a chemical material shows marked selective absorption in the infrared region. It is an important and non-destructive characterizing tool, which provides qualitative information regarding structural details of crystalline and non-crystalline substances, the position of ions in the crystal, local symmetry and the ordering phenomena<sup>23</sup>. The FT-IR spectra absorption bands mainly appear due to the vibrations of the oxygen ions with the cations producing various frequencies of the unit cell. Various absorption bands exist in FT-IR spectrum from functional groups and their linkages can be explored, are found to be dependent on atomic mass, cation radius, cation-anion bond distances, cation distribution *etc*<sup>23</sup>. Therefore, FT-IR spectra indicate to the valance state of the ions and their occupation in the spinel lattice crystal. The electrical and magnetic properties of spinels depend on the chemical composition, cation distribution and the method of preparation. The vibrational, electronic and magnetic dipole spectra can give information about the position and valency of the ions in the crystal lattice<sup>19</sup>. In a certain mixed spinel ferrites, as the concentration of the divalent metal ions increasing, it gives rise to the structural change in spinel lattice crystal without affecting the spinel ferrite structure<sup>21</sup>. The structural changes brought about by the metal ions that are either lighter or heavier than divalent ions in the ferrites, which strongly influence the lattice vibrations. The vibration frequency depends on the cations mass, the cations oxygen distance and the bonding-force<sup>22</sup>.

The room temperature FT-IR spectra of the prepared  $\text{Ni}_{1-x}\text{Zn}_x\text{Fe}_2\text{O}_4$  samples were recorded between the wave numbers  $350 \text{ cm}^{-1}$  to  $1000 \text{ cm}^{-1}$ , which is a common feature of ferrites as shown in Figure 2. The measured FT-IR spectra confirm the formation of a single phase of spinel ferrites having two sites  $T_d$  and  $O_h$  of spinel structure. Here in, two prominent bands are present two different wave numbers  $\nu_T$  and  $\nu_O$ . The higher wave number,  $\nu_T$ , band lies between  $550 \text{ cm}^{-1}$  to  $600 \text{ cm}^{-1}$  corresponding to the highest restoring force, which is attributed to the stretching vibrations of metal-oxygen (*M-O*) bond in  $T_d$  group complexes. The lower wave number,  $\nu_O$ , at around  $400 \text{ cm}^{-1}$  is caused by the intrinsic vibrations of *M-O* bond in  $O_h$  group complexes. This is a good agreement with the observation by many researchers for various spinel materials<sup>19,24-29</sup>. The obtained FT-IR results confirm that the normal mode of vibration of  $T_d$  cluster is higher than that of  $O_h$  cluster<sup>30</sup>. The difference in frequencies of the characteristic vibrations ( $\nu_T$  and  $\nu_O$ ) has been attributed to the long bond length of *M-O* ions in  $O_h$  sites and short bond length of *M-O* ions in  $T_d$  sites. The difference in band positions for  $T_d$  and  $O_h$  group complexes of spinel structure is due to the difference in values of *Fe-O* bond lengths<sup>19,20,27,28,31,32</sup>. It was also found that, the *Fe-O* bond distance of the  $T_d$  sites ( $0.189 \text{ nm}$ ) and this is smaller than that of the  $O_h$  sites ( $0.199 \text{ nm}$ )<sup>33</sup>. The change in the frequency band position is due to perturbation occurring in the *Fe-O* inter nuclear distances<sup>19,23</sup>. This has been interpreted due to the more covalent bonding of the *Fe* ions at  $T_d$  sites. The positions of absorption bands in terms of wave number  $\nu_T$  and  $\nu_O$  for all samples are summarized in Table 1.

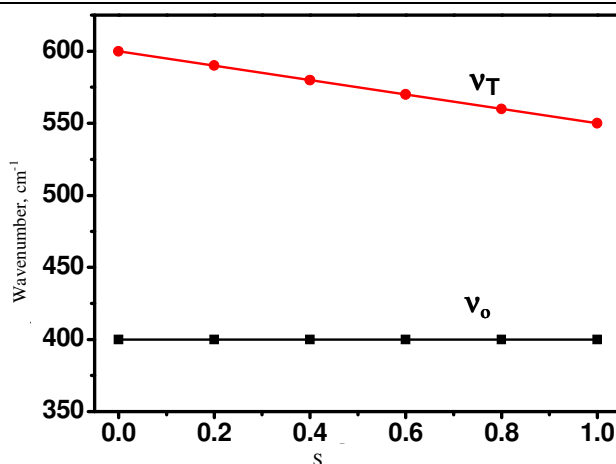
From Table 1, it is clear that only the position of  $\nu_T$  band is shifted with the incorporation of Zn ions in the Ni matrix. The same behavior was reported in previous work of different ferrite systems<sup>31,34</sup>. FT-IR results clearly indicate that Ni ions is stabilized in the  $O_h$  crystal field whereas Zn ions prefers  $T_d$  sites because of its ability to form covalent bonds<sup>10,25,26,35</sup>.



**Figure 2.** FT-IR absorption spectra of the mixed  $Ni_{1-x}Zn_xFe_2O_4$  spinel ferrite

**Table 1.** Absorption bands frequency for  $T_d$ ,  $O_h$  and  $\nu_{th}$  positions for the prepared mixed  $Ni_{1-s}Zn_sFe_2O_4$  spinel ferrite samples

$s$	$\nu_T \text{ cm}^{-1}$	$N_O \text{ cm}^{-1}$	$\nu_{th} \text{ cm}^{-1}$
0.0	600	400	755
0.2	590	400	760
0.4	580	400	765
0.6	570	400	770
0.8	560	400	775
1.0	550	400	780

**Figure 3.** The positions of  $\nu_T$  and  $\nu_O$  with respect to the Zn ratio”  $s$ ”

The calculated values of the force constant  $F_{CT}$  and  $F_{CO}$  for  $T_d$  and  $O_h$  sites, respectively, are listed in Table 2 using the following relation<sup>31</sup>

$$F_C = 4\pi^2 c^2 \nu^2 m \quad (1)$$

where

$c$  is the light velocity  $\approx 2.99 \times 10^{10} \text{ cm. sec}^{-1}$

$\nu$  is the vibration frequency of  $T_d$  and  $O_h$  sites.

$M$  is the reduced mass of Fe and O ions, which is found  $\approx 2.061 \times 10^{-23} \text{ g}$ .

**Table 2.** Calculated values of the force constant  $F_{CT}$  and  $F_{CO}$  or the mixed  $Ni_{1-s}Zn_sFe_2O_4$  spinel ferrite

$s$	$F_{CT} \times 10^5, \text{ dyne.cm}^{-1}$	$F_{CO} \times 10^5, \text{ dyne.cm}^{-1}$
0.0	2.61	1.16
0.2	2.53	1.16
0.4	2.43	1.16
0.6	2.36	1.16
0.8	2.28	1.16
1.0	2.20	1.16

Since the applied vibration frequency is proportional to the force constant  $F_C$ , so  $\nu_T$  shift of the Fe-O bond vibration to lower frequency with increasing of the Zn ions. This indicates that,  $F_C$  of the Fe-O bond decreasing in the mixed  $Ni$ - $Zn$  spinel ferrite. The observed change

in  $\nu_T$  and decrease in  $F_{CT}$  indicate the occupancy of Zn ions at  $T_d$  sites<sup>19</sup>. The results show the compositional dependent behavior of force constant are attributed to the cation oxygen bond distances<sup>1</sup>. It is attributed to the shorter bond length of  $T_d$  cluster and longer bond length of  $O_h$  cluster<sup>29</sup>. Normally, it is expected that an increase in bond length should lead to a decrease in force constant. If the radius of the impurity ion is larger than the displaced ion then the bond length increases, lowering the force constant for either site or a reduction in the repulsive forces between the ions leading to a lower electrostatic energy implying lower wave number. Reverse will hold if a smaller impurity ion replaces a metal ion of the regular lattice. A decrease in wave number and force constant is expected with  $Zn^{2+}$  ion substitution because of its larger ionic radius than the displaced  $Zi^{2+}$  ion.

The FT- IR spectra of the composition  $Ni_{1-s}Zn_sFe_2O_4$  shows a change in the absorption bands by introducing the Zn ions, which has larger ionic radius and higher atomic weight, on the  $T_d$  sites. This tends to increase the ionic radius of the  $T_d$  sites with addition of the Zn ions<sup>32</sup>. This is attributed to the method of preparation, the grains size and the porosity that influences the band position<sup>20,21,28</sup>. This affects Fe-O bond-stretching vibration<sup>36</sup>. Therefore, there are slight shift towards low frequency side in the  $\nu_T$  band.

The threshold frequency ( $\nu_{th}$ ), according to Waldron<sup>28</sup> for the electronic transition can be determined from the maximum point in the absorption spectra, where it reaches a limiting value as in Figure 3. The values of threshold frequency  $\nu_{th}$  are in Table 1, which are shown in Figure 4. It is noticed that,  $\nu_{th}$  is increasing with the increase of Zn ions content. This increment in  $\nu_{th}$  is not reflected on the value of the corresponding activation energy  $E_a$ . Which is calculated from the relation  $E_{th}=h\nu_{th}$  that has a constant average value about 0.1 eV, where h is Planck's constant.

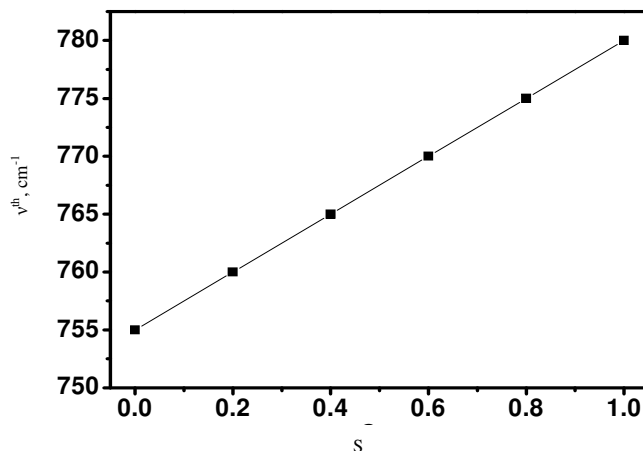
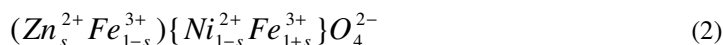


**Figure 4.** Variation of  $\nu_{th}$  with the Zn ratio " s "

It is necessary to know the cations distribution, which could be described with the following considerations.



The non-magnetic Zn ions occupy the  $T_d$  sites, which are favored by the polarization effect and this occurs by replacing the Fe ions in the  $T_d$  sites. However, the  $T_d$  sites preferences of the cations depend upon their electronic configuration<sup>38</sup>. The Zn ions show a marked stronger preference for the  $T_d$  sites than the Fe ions, where their (4s 3d) electrons form a covalent bonds with 2p electrons of the oxygen ion<sup>38,39</sup>.

Depending on the cations distribution that is given in the considered cations distribution, the ionic radii for  $T_d$  and  $O_h$  sites, we used the following equations<sup>40,41</sup>

$$R_T = sR_{Zn^{2+}} + (1-s)R_{Fe^{3+}} \quad (3)$$

$$R_O = \frac{1}{2}[(1-s)R_{Ni^{2+}} + (1+s)R_{Fe^{3+}}] \quad (4)$$

where

$R_T$  and  $R_O$  are the mean ionic radii per molecule for  $T_d$  and  $O_h$  sites, respectively.

$R_{Zn^{2+}}$  is the ionic radius of the Zn ion.

$R_{Fe^{2+}}$  is the ionic radius of the Fe ion.

$R_{Ni^{2+}}$  is the ionic radius of the Fe ion.

The ionic radii  $R_T$  and  $R_O$  versus the Zn ratio "s" are plotted in Figure 5, while  $R_T/R_O$  versus the Zn ratio "s" is plotted in Figure 6. It is noticed that, with increasing of the  $Zn^{2+}$  ions  $R_T$  increases while  $R_O$  decreases. This behavior is attributed to the replacement of the Fe ions with the large ionic radius of the Zn ions on  $T_d$  sites and Ni ions with the smaller ionic radius than Fe ions on  $O_h$  sites. The cations distribution, the calculated ionic radii  $R_T$  and  $R_O$  and ionic ratio  $R_T/R_O$  are tabulated in Table 3.

**Table 3.** Values of  $R_T$ ,  $R_O$  and  $R_T/R_O$  for the mixed Ni-Zn spinel ferrite

s	Cations distribution	$R_T$ , nm	$R_O$ , nm	$R_T/R_O$
0.0	$(Fe_{1.0}^{3+})\{Ni_{1.0}^{2+}Fe_{1.0}^{3+}\}O_4^{2-}$	0.063	0.076	0.82894
0.2	$(Zn_{0.2}^{2+}Fe_{0.8}^{3+})\{Ni_{0.8}^{2+}Fe_{1.2}^{3+}\}O_4^{2-}$	0.0652	0.0746	0.87399
0.4	$(Zn_{0.4}^{2+}Fe_{0.6}^{3+})\{Ni_{0.6}^{2+}Fe_{1.4}^{3+}\}O_4^{2-}$	0.0674	0.0732	0.92076
0.6	$(Zn_{0.6}^{2+}Fe_{0.4}^{3+})\{Ni_{0.4}^{2+}Fe_{1.6}^{3+}\}O_4^{2-}$	0.0696	0.0718	0.96935
0.8	$(Zn_{0.8}^{2+}Fe_{0.2}^{3+})\{Ni_{0.2}^{2+}Fe_{1.8}^{3+}\}O_4^{2-}$	0.0718	0.0704	1.01988
1.0	$(Zn_{1.0}^{2+})\{Fe_{2.0}^{3+}\}O_4^{2-}$	0.074	0.069	1.07246

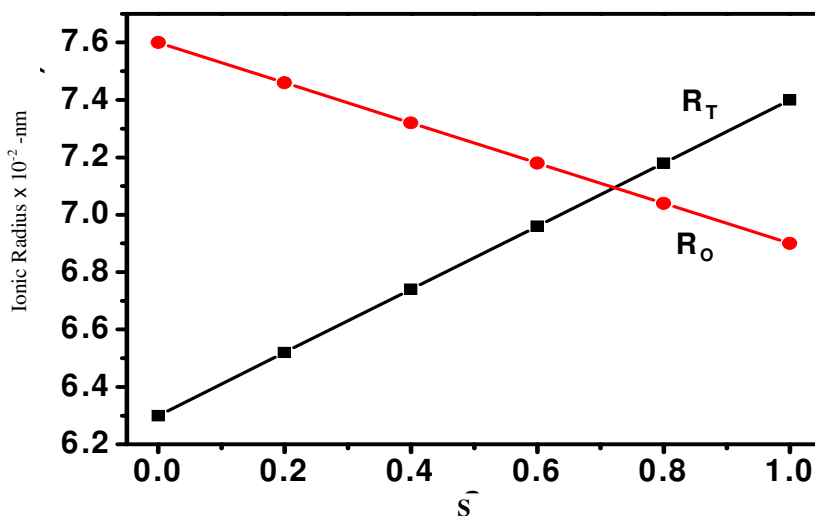


**Figure 5.** Variation of  $R_T$  and  $R_O$  with the Zn ratio "s"

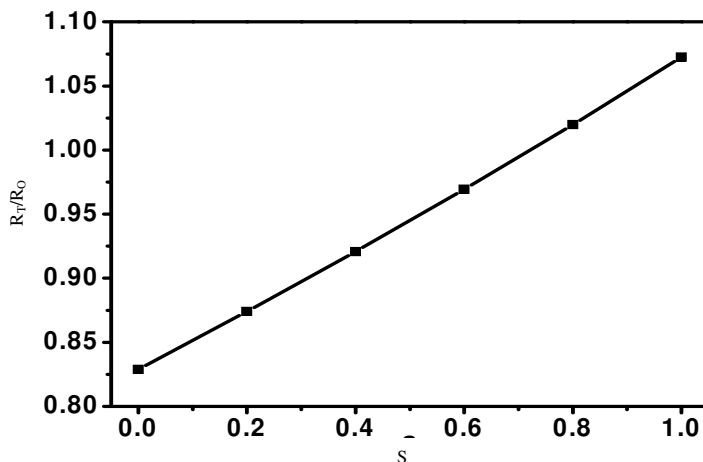


Figure 6. Variation of  $R_T/R_O$  with the Zn ratio " s "

## Conclusion

FT-IR spectra of the diamagnetic Zn ions substituted on the Ni spinel ferrite have been analyzed in the frequency range (350-1000)  $\text{cm}^{-1}$ . Two bands were observed, their positions were found to depend, strongly, on Zn ions content.

1. FT-IR spectra indicated that two main prominent bands are detected, one of a high frequency band  $\nu_T$  at around (550-600)  $\text{cm}^{-1}$  and the other of a low frequency band  $\nu_O$  at 400  $\text{cm}^{-1}$  and are assigned to  $T_d$  and  $O_h$  sites, respectively.
2. Force constant  $F_C$  of  $T_d$  and  $O_h$  sites were calculated and found to decrease with increasing the Zn ions.
3. On the basis of analyzing the FT-IR absorption bands, we deduced the cations distribution for the given mixed ferrite as the following form  $(Zn_s^{2+}Fe_{1-s}^{3+})\{Ni_{1-s}^{2+}Fe_{1+s}^{3+}\}O_4^{2-}$ . This illustrated that the non-magnetic Zn ions has a preference to  $T_d$  sites, where the Ni ions occupy  $O_h$  sites.
4. The ionic radii of  $T_d$  and  $O_h$  sites were calculated and found to change linearly with increasing the Zn ions.

## Acknowledgment

The authors are grateful to the staff of Chemistry Department, at the Islamic University-Gaza, for their help during this work.

## References

1. Kumar K V, Sridhar R, Ravinder D and Krishna K R, *IJAPM*, 2014, **4(2)**, 113-117; DOI:10.7763/IJAPM.2014.V4.265
2. Yahya N, Aripin A S M N, Aziz A A, Daud H, Zaid H M, Pah L K and Maarof N, *AJEAS*, 2008, **1(1)**, 53-56; DOI:10.3844/ajeassp.2008.53.56
3. Al-Aaraj B, *Tishreen University Journal for Research and Scientific Studies - Basic Sciences Series*, 2008, **30(4)**, 167-206.
4. Shaat S K K, Swart H C and Ntwaeaborwa O M, *J Alloys Compd.*, 2014, **587**, 600-605; DOI:10.1016/j.jallcom.2013.11.001
5. Shaat S K K, Swart H C and Ntwaeaborwa O M, *SAIP*, 2013, ISBN: 978-0-620-62819-8.



6. Carballal D S, Roldan A, Crespo R G and Leeuw N H, *Phys Rev B: Condens Matter.*, 2015, **91(19)**, 195106.
7. Chau N, Thuan N K, Minh D L and Luong N H, *VNU J Sci, Mathemat- Phys.*, 2008, **24**, 155-162.
8. Cabanas A and Poliakoff M, *J Mater Chem.*, 2001, **11**, 1408-1416; DOI:10.1039/B009428P
9. Shaath S K K, Advanced Ferrite Technology, Lambert Academic Publishing, 2012,
10. Singh S, Singh M, Ralhan N K, Kotnala R K and Verma K C, *Adv Mat Lett.*, 2012, **3(6)**, 504-506; DOI:10.5185/amlett.2012.icnano.226
11. Shahjahan M, Ahmed N A, Rahman S N, Islam S and Khatun N, *IJETCAS*, 2014, **13(104)**, 20-25.
12. Akhtar M N, Yahya N and Hussain P B, *IJBAS-IJENS*, 2009, **09(09)**, 37-40.
13. Ma R, Wang Y, Tian Y, Zhang C and Li X, *J Mater Sci Technol.*, 2008, **24(3)**, 419-422.
14. Krishna K R, Kumar K V, Ravindernathgupta C and Ravinder D, *Adv Mater Phys Chem.*, 2012, **2**, 149-154; DOI:10.4236/ampc.2012.23022
15. Kumar S, Sharma A, Singh M and Sharma S P, *Arch Appl Sci Res.*, 2013, **5(6)**, 145-151.
16. Krishna K R, Kumar K V and Ravinder D, *Adv Mater Phys Chem.*, 2012, **2(3)**, 185-191; DOI:10.4236/ampc.2012.23028
17. Kurmude D V, Barkule R S, Raut A V, Shengule D R and Jadhav K M, *J Supercond Nov Magn.*, 2013, **27(2)**, 547-553; DOI:10.1007/s10948-013-2305-2
18. Soibam I, Nilima N and Phanjobam S, *Am J Mater Sci Engg*, 2014, **2(2)**, 24-27; DOI:10.12691/ajmse-2-2-3
19. Raju M K, *Chem Sci Trans.*, 2015, **4(1)**, 137-142; DOI:10.7598/cst2015.957
20. Carta D, Casula M F, Falqui A, Loche D, Mountjoy G, Sangregorio C and Corrias A, *J Phys Chem C*, 2009, **113(20)**, 8606-8615; DOI:10.1021/jp901077c
21. Reddy P V and Salagram M, *Phys Stat Sol (A)*, 1987, **100(2)**, 639-643; DOI:10.1002/pssa.2211000230
22. Patil A A, Otari S M, Mahajan V C, Patil M G, Patil A B, Soudagav B K, Patil B L and Sawant S R, *Sol Stat Comm.*, 1991, **78(1)**, 39-42; DOI:10.1016/0038-1098(91)90805-6
23. Khot S S, Shinde N S, Ladgaonkar B, Kale B B and Watawe S C, *IJAET*, 2011, **1(4)**, 422-429.
24. Shaath S K K, Swart H C and Ntwaeaborwa O M, *J Electron Spectro Relat Phenom.*, 2014, **197**, 72-79; DOI:10.1016/j.elspec.2014.09.012
25. Dawoud H, *J Al-Aqsa Univ.*, 2006, **10(S.E.)**, 247-262.
26. Venkataraju C and Paulsingh R, *J Nanoscience*, 2014, **2014**, 1-5; DOI:10.1155/2014/815385
27. Dixit G, Singh J P, Srivastava R C, Agrawal H M and Chaudhary R J, *Adv Mat Lett.*, 2012, **3(1)**, 21-28; DOI:10.5185/amlett.2011.6280
28. Waldron R D, *Phys Rev.*, 1955, **99(6)**, 1727-1734; DOI:10.1103/PhysRev.99.1727
29. Hanfner S, *Z kristallogr*, 1961, **115(5-6)**, 331-358.
30. Naidu V, Ahamed S K A, Dawood M S and Suganthi M, *Int J Com Appl.*, 2011, **24(2)**, 18-22; DOI:10.5120/2923-3862
31. Mazen S A, Abed Allah M A, Nakhla R I and Zaki H M, *Mat Chem Phys.*, 1993, **34(1)**, 35-40; DOI:10.1016/0254-0584(93)90116-4
32. Shaikh A M, Jadhav S A, Watawe S C and Chongnle B K, *Mat Lett.*, 2000, **44(3-4)**, 192-196; DOI:10.1016/S0167-577X(00)00025-2
33. Evans B J and Hanfner S S, *J Phys Chem Solids*, 1968, **29(9)**, 1573-1588; DOI:10.1016/0022-3697(68)90100-5

34. Mazen S A, Hakeem N A and Sabrah B A, *Phys Status Sol., (b)*, 1984, **123(1)**, K1-K4; DOI:10.1002/pssb.2221230141
35. Battoo K M and Ansari M S, *Nanoscale Research Letters*, 2012, **7(112)**, 2-14; DOI:10.1186/1556-276X-7-112
36. Mazen S A, *Mat Chem Phys.*, 2000, **62(2)**, 139-147; DOI:10.1016/S0254-0584(99)00158-3
37. Vishwanathan B and Murthy V R K, *Ferrites Materials, Sci Technol.*, 1990.
38. Xioa-Xia T, Manthiram A and Good-enough G B, *J Sol State Chem.*, 1989, **79(2)**, 250-262; DOI:10.1016/0022-4596(89)90272-7
39. Belled S S, Pujar R B and Chougule B K, *Mat Chem Phys.*, 1998, **52**, 166-169; DOI:10.1016/S0254-0584(98)80019-9
40. Potakova V A, Zvera N D and Romanov V P, *Phys Stat Sol., (A)*, 1972, **12(1)**, 623-627; DOI:10.1002/pssa.2210120235
41. Standly K J, *Oxide Magnetic Materials*, Clarendon Press Oxford, 1972.